COVID-19 Crisis Reduces Free Tropospheric Ozone across the Northern Hemisphere

Wolfgang Steinbrecht, Dagmar Kubistin, Christian Plass-Dülmer, Jonathan Davies, David W. Tarasick, Peter von Der Gathen, Holger Deckelmann, Nis Jepsen, Rigel Kivi, Norrie Lyall, et al.

COVID-19 Crisis Reduces Free Tropospheric Ozone across the Northern Hemisphere

Wolfgang Steinbrecht[1], Dagmar Kubistin[1], Christian Plass-Dülmer[1], Jonathan Davies[2], David W. Tarasick[2], Peter von der Gathen[3], Holger Deckelmann[3], Nis Jepsen[4], Rigel Kivi[5], Norrie Lyall[6], Matthias Palm[7], Justus Notholt[7], Bogumil Kois[8], Peter Oelsner[9], Marc Allaart[10], Ankie Piters[10], Michael Gill[11], Roeland Van Malderen[12], Andy W. Delcloo[12], Ralf Sussmann[13], Emmanuel Mahieu[14], Christian Servais[14], Gonzague Romanens[15], Rene Stübi[15], Gerard Ancellet[16], Sophie Godin-Beekmann[16], Shoma Yamanouchi[17], Kimberly Strong[17], Bryan Johnson[18], Patrick Cullis[18, 19], Irina Petropavlovskikh[18, 19], James W. Hannigan[20], Jose-Luis Hernandez[21], Ana Diaz Rodriguez[21], Tatsumi Nakano[22], Fernando Chouza[23], Thierry Leblanc[23], Carlos Torres[24], Omaira Garcia[24], Amelie N. Röhling[25], Matthias Schneider[25], Thomas Blumenstock[25], Matt Tully[26], Clare Paton-Walsh[27], Nicholas Jones[27], Richard Querel[28], Susan Strahan[29,30], Ryan M. Stauffer[29,33], Anne M. Thompson[29], Antje Inness[31], Richard Engelen[31], Kai-Lan Chang[32,19], Owen R. Cooper[32,19]

[1]Deutscher Wetterdienst, Hohenpeißenberg, Germany.

[2]Environment and Climate Change Canada, Toronto, Canada.

[3]Alfred Wegener Institut, Helmholtz-Zentrum für Polar- und Meeresforschung, Potsdam, Germany.

[4]Danish Meteorological Institute, Copenhagen, Denmark.

[5]Finnish Meteorological Institute, Sodankylä, Finland.

[6]British Meteorological Service, Lerwick, United Kingdom.

[7]University of Bremen, Bremen, Germany.

[8]Institute of Meteorology and Water Management, Legionowo, Poland.

[9]Deutscher Wetterdienst, Lindenberg, Germany.

[10]Royal Netherlands Meteorological Institute, DeBilt, The Netherlands.

[11]Met Éireann (Irish Met. Service), Valentia, Ireland.

[12]Royal Meteorological Institute of Belgium, Uccle, Belgium.

[13]Karlsruhe Institute of Technology, IMK-IFU, Garmisch-Partenkirchen, Germany.

[14]Institute of Astrophysics and Geophysics, University of Liège, Liège, Belgium.

[15]Federal Office of Meteorology and Climatology, MeteoSwiss, Payerne, Switzerland.

[16]LATMOS, Sorbonne Université-UVSQ-CNRS/INSU, Paris, France.

[17]University of Toronto, Toronto, Canada.

[18]NOAA ESRL Global Monitoring Laboratory, Boulder, CO, USA.

[19]Cooperative Institute for Research in Environmental Sciences (CIRES), University of Colorado, Boulder, CO, USA.

This article has been accepted for publication and undergone full peer review but has not been through the copyediting, typesetting, pagination and proofreading process, which may lead to differences between this version and the Version of Record. Please cite this article as doi: 10.1029/2020GL091987.

[20]National Center for Atmospheric Research, Boulder, CO, USA.

[21]State Meteorological Agency (AEMET), Madrid, Spain.

[22]Meteorological Research Institute, Tsukuba, Japan.

[23]Jet Propulsion Laboratory, California Institute of Technology, Table Mountain Facility, Wrightwood, CA, USA.

[24]Izaña Atmospheric Research Center, AEMET, Tenerife, Spain.

[25]Karlsruhe Institute of Technology, IMK-ASF, Karlsruhe, Germany.

[26]Bureau of Meteorology, Melbourne, Australia.

[27]Centre for Atmospheric Chemistry, University of Wollongong, Wollongong, Australia.

[28]National Institute of Water and Atmospheric Research, Lauder, New Zealand.

[29]Earth Sciences Division, NASA Goddard Space Flight Center, Greenbelt, MD, USA.

[30]Universities Space Research Association, Columbia, MD, USA.

[31]European Centre for Medium-Range Weather Forecasts, Reading, United Kingdom.

[32]NOAA Chemical Sciences Laboratory, Boulder, CO, USA.

[33]Earth System Science Interdisciplinary Center, University of Maryland, College Park, MD, USA

Corresponding author: Wolfgang Steinbrecht (wolfgang.steinbrecht@dwd.de)

Key Points (shortened to less than 140 characters each, and changed as suggested by Reviewer #2):

- In spring and summer 2020, stations in the northern extratropics report on average 7% (4 nmol/mol) less tropospheric ozone than normal.
- Such low tropospheric ozone, over several months, and at so many sites, has not been observed in any previous year since at least 2000.
- Most of the reduction in tropospheric ozone in 2020 is likely due to emissions reductions related to the COVID-19 pandemic.

Abstract

Throughout spring and summer 2020, ozone stations in the northern extratropics recorded unusually low ozone in the free troposphere. From April to August, and from 1 to 8 kilometers altitude, ozone was on average 7% (≈4 nmol/mol) below the 2000 to 2020 climatological mean. Such low ozone, over several months, and at so many stations, has not been observed in any previous year since at least 2000. Atmospheric composition analyses from the Copernicus Atmosphere Monitoring Service and simulations from the NASA GMI model indicate that the large 2020 springtime ozone depletion in the Arctic stratosphere contributed less than one quarter of the observed tropospheric anomaly. The observed anomaly is consistent with recent chemistry-climate model simulations, which assume emissions reductions similar to those caused by the COVID-19 crisis. COVID-19 related emissions reductions appear to be the major cause for the observed reduced free tropospheric ozone in 2020.

Plain Language Summary

Worldwide actions to contain the COVID-19 virus have closed factories, grounded airplanes, and have generally reduced travel and transportation. Less fuel was burnt, and less exhaust was emitted into the atmosphere. Due to these measures, the concentration of nitrogen oxides and volatile organic compounds (VOCs) decreased in the atmosphere. These substances are important for photochemical production and destruction of ozone in the atmosphere. In clean or mildly polluted air, reducing nitrogen oxides and/or VOCs will reduce the photochemical production of ozone and result in less ozone. In heavily polluted air, in contrast, reducing nitrogen oxides can increase ozone concentrations, because less nitrogen oxide is available to destroy ozone. In this study, we use data from three types of ozone instruments, but mostly from ozonesondes on weather balloons. The sondes fly from the ground up to 30 kilometers altitude. In the first 8 kilometers, we find significantly reduced ozone concentrations in the northern extratropics during spring and summer of 2020, less than in any other year since at least 2000. We suggest that reduced emissions due to the COVID-19 crisis have lowered photochemical ozone production and have caused the observed ozone reductions in the troposphere.

1 Introduction

Widespread measures to contain the COVID-19 pandemic have slowed, or even closed down, industries, businesses, and transportation activities, and have reduced anthropogenic emissions substantially throughout the year 2020. Guevara et al. (2020), or Barré et al. (2020) report European emissions reductions up to 60% for NO_x, and up to 15% for Non-Methane Volatile Organic Compounds (NMVOC) in March/April 2020. Based on satellite observations of NO_2 columns (Bouwens et al., 2020), comparable NO_x emissions reductions are reported for Chinese cities in February 2020 (Ding et al., 2020; Feng et al., 2020). Globally averaged CO_2 emissions decreased by 8.8% during the first half of 2020 (Liu et al., 2020), consistent in timing and magnitude with the aforementioned NO_2 emission reductions. The largest relative reductions occurred for air traffic, where emissions decreased by ≈40%, on average, in the first half of 2020 (Le Quéré et al., 2020a; Liu et al., 2020), and remained low during the second half of 2020 (Le Quéré et al., 2020b).

These COVID-19 emissions reductions are large enough to affect ozone levels in the troposphere (Dentener et al., 2011). Tropospheric O_3-NO_x-VOC-HO_x chemistry is, however, complex and nonlinear. The net effect of emission changes depends on NO_x and VOC concentrations (e.g., Kroll et al., 2020; Sillman, 1999; Thornton et al., 2002). In polluted regions, at high NO_x concentrations (>> 1pbb), reducing NO_x concentrations can increase ozone, because ozone titration by NO is reduced (e.g., Sicard et al., 2020). At low concentrations (NO_x < 1 nmol/mol), however, in the clean or mildly polluted free troposphere, reducing NO_x lowers photochemical ozone production (e.g., Bozem et al., 2017), and results in less ozone.

Indeed, for many polluted regions, studies report increased near-surface ozone after COVID-19 lockdowns (e.g., Collivignarelli et al., 2020; Lee et al., 2020; Shi & Brasseur, 2020; Siciliano et al., 2020; Venter et al., 2020). Reduced surface ozone is reported for some rural areas, e.g., in the US and Western Europe (Chen et al., 2020; Menut et al., 2020). Meteorological conditions complicate matters, as they play an important role as well (Goldberg et al., 2020; Keller et al., 2021; Ordóñez et al., 2020; Shi & Brasseur, 2020).

In the free troposphere, ozone is an important greenhouse gas, and plays a key role in tropospheric chemical reactions, controlling the oxidizing capacity (e.g. Archibald et al., 2020; Cooper et al., 2014; Gaudel et al, 2018). The Northern Hemisphere free troposphere is dominated by net photochemical ozone production, proportional (albeit nonlinearly) to the availability of ozone precursor gases (e.g., Zhang et al., 2020). In contrast to increases of surface ozone in polluted urban areas after the COVID-19 emissions reductions, we find significant reductions of ozone in the northern extratropical free troposphere. These large-scale reductions occurred in late spring and summer 2020, following the widespread COVID-19 slowdowns, and are unique within the last two decades.

2 Instruments and Data

Regular observations of ozone in the free troposphere are sparse: Only around 50 ozone sounding stations worldwide (e.g. Tarasick et al., 2019), a handful of tropospheric lidars (Gaudel et al., 2015; Leblanc et al., 2018), and about twenty Fourier Transform Infrared Spectrometers (FTIRs, Vigouroux et al., 2015). In-Service Aircraft for a Global Observing System (IAGOS, Nédélec et al., 2015) are another important source of tropospheric ozone data. Due to the COVID-19 slowdowns, however, few IAGOS aircraft were flying in 2020, and IAGOS data became quite sparse, with only about 20 flights per month since April 2020, compared to more than 200 flights per month in 2019. The information content of satellite measurements on ozone in the free troposphere is limited, and accuracy is modest, 10 to 30% (Hurtmans et al., 2012; Liu et al., 2010; Oetjen et al., 2014). The recent Tropospheric Ozone Assessment Report found large differences in tropospheric ozone trends derived from different satellite instruments, and even different signs in some regions (Gaudel et al., 2018).

Ozonesondes measure profiles with high vertical resolution, about 100 m, and good accuracy, 5 to 15% in the troposphere, 5% in the stratosphere (Smit et al., 2007; Sterling et al., 2018; Tarasick et al., 2016; Van Malderen et al., 2016; Witte et al., 2017; WMO, 2014). This is adequate to detect ozone anomalies of several percent. We use stations with regular soundings, at least once per month since the year 2000, and with data available until at least July 2020. Soundings with obvious deficiencies were rejected (i.e. large data gaps, integrated ozone column from the sounding deviating by more than 30% from ground- or satellite-based spectrometer measurement). Table 1 provides information on stations, and public data archives.

Table 1. Stations in this study, mostly ozonesonde stations. *FTIR and LIDAR stations are italicized*. Data sources: **W**=World Ozone and UV Data Centre (https://woudc.org/archive/Archive-NewFormat/OzoneSonde_1.0_1/), **N**=Network for the Detection of Atmospheric Composition Change (ftp://ftp.cpc.ncep.noaa.gov/ndacc/station/; ftp://ftp.cpc.ncep.noaa.gov/ndacc/RD/), **E**= European Space Agency Validation Data Center (https://evdc.esa.int/ requires registration, or ftp://zardoz.nilu.no/nadir/projects/vintersol/data/o3sondes requires account), **G**=Global Monitoring Laboratory, National Oceanic and Atmospheric Administration (ftp://aftp.cmdl.noaa.gov/data/ozwv/Ozonesonde/)

[1] Due to COVID-19 restrictions, most Canadian ozonesonde data were available only up to March or April 2020.

[2] Tateno data were corrected for the change from Carbon Iodine to ECC ozonesondes in December 2009.

[3] Stations affected by a drop-off in ECC sonde sensitivity > 3% in the stratosphere, after 2015 (see Stauffer et al., 2020). The drop-off is much smaller (<< 1%) in the troposphere, and should be negligible here. At many of the affected stations, ECC sondes behaved normally again in 2019/2020.

Station	**Latitude (deg N)**	**Longitude (deg E)**	**Data source (see caption)**	**Data until**	**Profiles / spectra per month in 2020**
Alert, Canada [1, 3]	82.50	-62.34	W	4/2020	3.75
Eureka, Canada [3]	80.05	-86.42	W, E	9/2020	4.89
Ny-Ålesund, Norway	78.92	11.92	W, E	10/2020	7.10
Ny-Ålesund FTIR, Norway	*78.92*	*11.92*	*N*	*7/2020*	*12.86*
Thule FTIR, Greenland	*76.53*	*-68.74*	*N*	*9/2020*	*73*
Resolute, Canada [1]	74.72	-94.98	W	4/2020	5.50
Scoresbysund, Greenland	70.48	-21.95	E	11/2020	4.00
Kiruna FTIR, Sweden	*67.41*	*20.41*	*N*	*7/2020*	*46*
Sodankylä, Finland	67.36	26.63	W, E	12/2020	2.83
Lerwick, United Kingdom	60.13	-1.18	W, E	12/2020	3.92
Churchill, Canada [1, 3]	58.74	-93.82	W	3/2020	3.33
Edmonton, Canada [1, 3]	53.55	-114.10	W	3/2020	3.67
Goose Bay, Canada [1]	53.29	-60.39	W	3/2020	2.67
Bremen FTIR, Germany	*53.13*	*8.85*	*N*	*10/2020*	*5.27*
Legionowo, Poland	52.40	20.97	W	10/2020	4.00
Lindenberg, Germany	52.22	14.12	W	11/2020	4.73
DeBilt, Netherlands	52.10	5.18	W, E	12/2020	4.33
Valentia, Ireland	51.94	-10.25	W, E	12/2020	2.50

Uccle, Belgium	50.80	4.36	W, E	12/2020	12.00
Hohenpeissenberg, Germany	47.80	11.01	W	12/2020	10.50
Zugspitze FTIR, Germany	*47.42*	*10.98*	*N*	*9/2020*	*73*
Jungfraujoch FTIR, Switzerland	*46.55*	*7.98*	*N*	*12/2020*	*46*
Payerne, Switzerland	46.81	6.94	W	10/2020	11.10
Haute Provence, France	43.92	5.71	N	8/2020	2.50
Haute Provence LIDAR, France	*43.92*	*5.71*	*N*	*8/2020*	*3.50*
Toronto FTIR, Canada	*43.66*	*-79.40*	*N*	*10/2020*	*59*
Trinidad Head, California, USA	41.05	-124.15	G	12/2020	3.58
Madrid, Spain	40.45	-3.72	W	11/2020	4.09
Boulder, Colorado, USA	39.99	-105.26	G	12/2020	4.83
Boulder FTIR, Colorado, USA	*39.99*	*-105.26*	*N*	*10/2020*	*56*
Tateno (Tsukuba), Japan [2]	36.05	140.13	W	10/2020	2.70
Table Mountain LIDAR, California, USA	*34.40*	*-117.70*	*N*	*8/2020*	*19*
Izana, Tenerife, Spain	28.41	-16.53	W	8/2020	2.00
Izana FTIR, Tenerife, Spain	*28.30*	*-16.48*	*N*	*9/2020*	*28*
Hong Kong, China	22.31	114.17	W	9/2020	4.11
Hilo, Hawaii, USA [3]	19.72	-155.07	G	12/2020	4.08
Mauna Loa FTIR, Hawaii, USA	*19.54*	*-155.58*	*N*	*10/2020*	*36*
Paramaribo, Suriname	5.81	-55.21	N, E	10/2020	3.60
Pago Pago, American Samoa [3]	-14.25	-170.56	G	12/2020	3.08
Suva, Fiji [3]	-18.13	178.32	G	9/2020	1.44
Wollongong FTIR, Australia	*-34.41*	*150.88*	*N*	*10/2020*	*43*
Broadmeadows, Australia	-37.69	144.95	W	7/2020	4.29
Lauder, New Zealand	-45.04	169.68	W	10/2020	4.40
Lauder FTIR, New Zealand	*-45.04*	*169.68*	*N*	*10/2020*	*99*
Macquarie Island, Australia	-54.50	158.94	W	7/2020	4.29

Apart from the sondes, FTIR spectrometers from the Network for the Detection of Atmospheric Composition Change (NDACC, De Mazière et al., 2018) provide independent information, based on a completely different method (ground-based solar-infrared absorption spectrometry). The altitude resolution of FTIR ozone profiles in the troposphere is much coarser (5 to 10 km) than that of the sondes, while accuracy is similar, 5 to 10% (Vigouroux et al.,2015). Finally, we use data from tropospheric lidars (Gaudel et al., 2015, Granados-Muñoz & Leblanc 2016), which provide ozone profiles from ≈3 to 12 km altitude, with accuracy comparable to the sondes (5 to 10%; Leblanc et al., 2018), and slightly coarser altitude resolution (100 m to 2 km).

We also use global atmospheric composition re-analyses from the Copernicus Atmosphere Monitoring Service for the years 2003 to 2019, and operational analyses for the year

2020 (CAMS, Inness et al., 2019; see also Park et al., 2020). The CAMS data are taken at the grid-points closest to the stations in Table 1. The analyses (in 2020) are adjusted for the small average difference to the re-analyses in 2018 and 2019. CAMS (re-)analyses are based on meteorological fields, and assimilation of satellite observations of ozone and NO_2. However, for NO_2 the impact of the assimilation is small and frequently insignificant, so that tropospheric NO_x in CAMS is essentially controlled by the prescribed emissions (Inness et al., 2019). Similarly, the limited information content of current satellite measurements of tropospheric ozone means that tropospheric ozone in CAMS is also driven largely by the prescribed emissions (and the chemistry module). Stratospheric ozone, however, is constrained well by the assimilated satellite data. Thus, CAMS analyses account for the large Arctic stratospheric depletion in spring of 2020 (Manney et al., 2020; Wohltmann et al., 2020), for 2020 meteorological conditions, and for ozone transport, e.g. from the stratosphere to the troposphere (Neu et al., 2014). However, since they rely on "business as usual" emissions for 2020, the CAMS analyses do not account for the effects of COVID-19 emissions reductions in 2020 on tropospheric ozone (and NO_x).

3 Results

For selected stations, Fig. 1 presents the annual cycles of tropospheric ozone over the last 20 years, at 6 km, a representative altitude for the free troposphere. Monthly means (over 1-km wide layers) reduce synoptic meteorological variability and measurement noise, and focus on longer-term, larger-scale variations.

Payerne, Jungfraujoch, and Trinidad Head show an annual cycle with low ozone in winter and high ozone in summer. This is the case for most stations in the northern extratropics (Cooper et al., 2014; Gaudel et al., 2018; Parrish et al., 2020). Increased photochemical production due to more sunlight and warmer temperatures is the main driver for the summer ozone maximum in the northern extratropics (Wu et al., 2007; Archibald et al., 2020).

Figure 1 shows substantial yearly variability, but ozone levels are notably below average in 2020, at all four stations (thick red lines in Fig. 1). At Payerne and Jungfraujoch, and a number of other stations, monthly means in spring and summer 2020 were actually the lowest, or close to the lowest, since 2000. For context, the dark blue lines in Fig. 1 provide global CO_2 emission reductions due to the COVD-19 pandemic (Le Quéré et al., 2020b). Comparable reductions apply to global ozone precursor emissions (NO_x and VOCs). The (daily) emission reductions in Fig. 1 indicate that the largest effect for ozone might be expected after March 2020. However, Fig. 1 does not show any clear or close correspondence between unusual ozone monthly means in 2020 (red lines) and the emission reductions (dark blue lines).

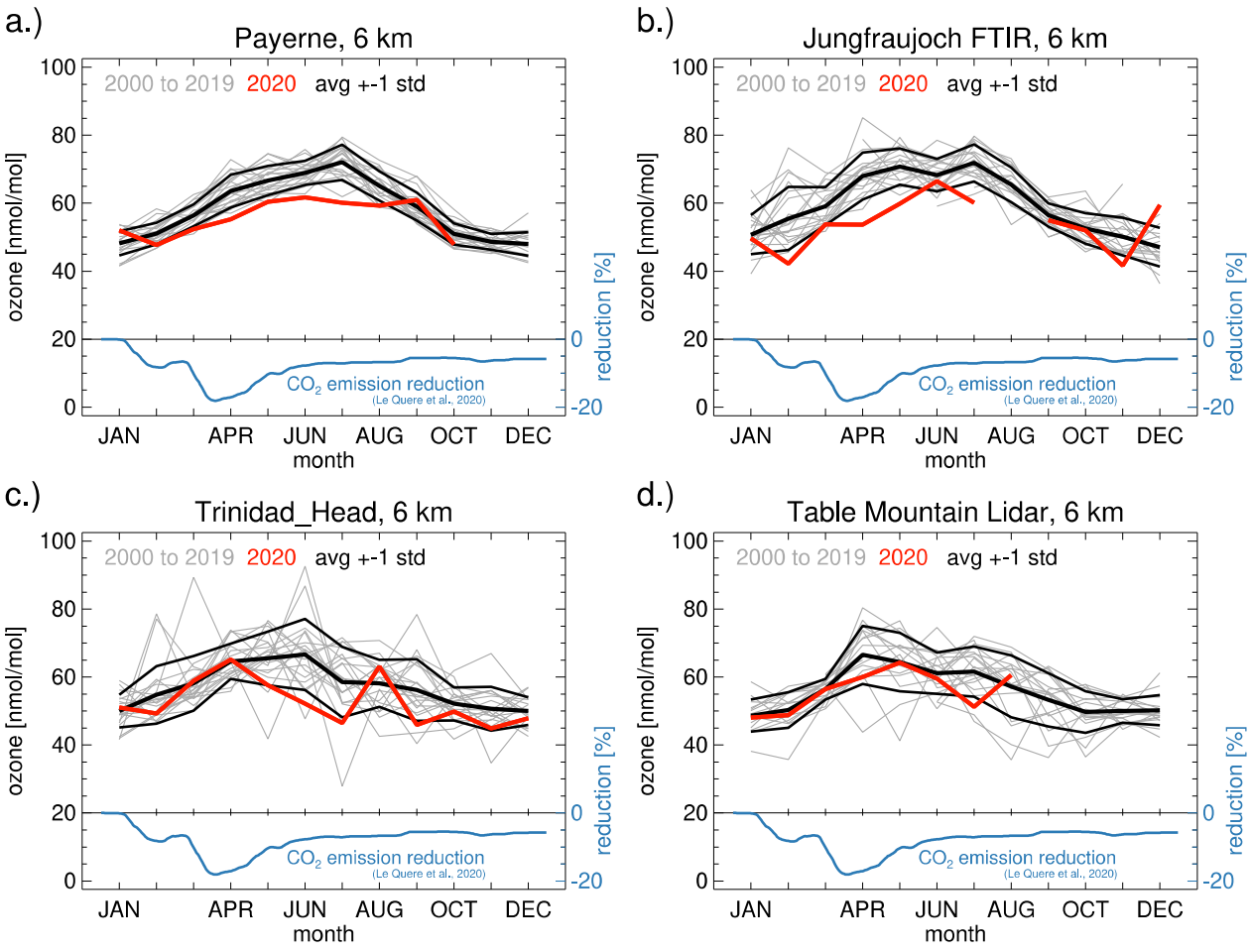

Figure 1. Observed ozone monthly means at four typical stations. Results are for 6 km altitude. The thick red line highlights the year 2020. Climatological averages, and standard deviations over the years 2000 to 2020 are indicated by the thick black lines. Payerne (**a**) and Trinidad Head (**c**) are sonde stations. Jungfraujoch (**b**) is an FTIR station. Table Mountain (**d**) is a lidar station. Dark blue lines and scale on the right: CO_2 emission reduction (in percent) from Le Quéré et al. (2020b), as a proxy for ozone precursor reductions in 2020.

Annual cycles of ozone anomalies, averaged over all northern extratropical stations (stations north of 15°N), are shown in Fig. 2. Anomalies were defined as the relative deviation (in percent) from the 2000-2020 climatological mean of each calendar month at each station. As for the single stations in Fig. 1, the observed northern extratropical average shows exceptionally low ozone throughout spring and summer 2020 (red line in Fig. 2a). This is not reproduced by the CAMS analyses, which do not account for COVID-19 related emissions reductions, and simulate ozone in the usual range in 2020 (red line in Fig. 2b). Again, there is no close temporal correspondence between the unusual behavior of observed ozone in 2020 (red line in Fig. 2a), and the emission reductions (dark blue line in Fig. 2a).

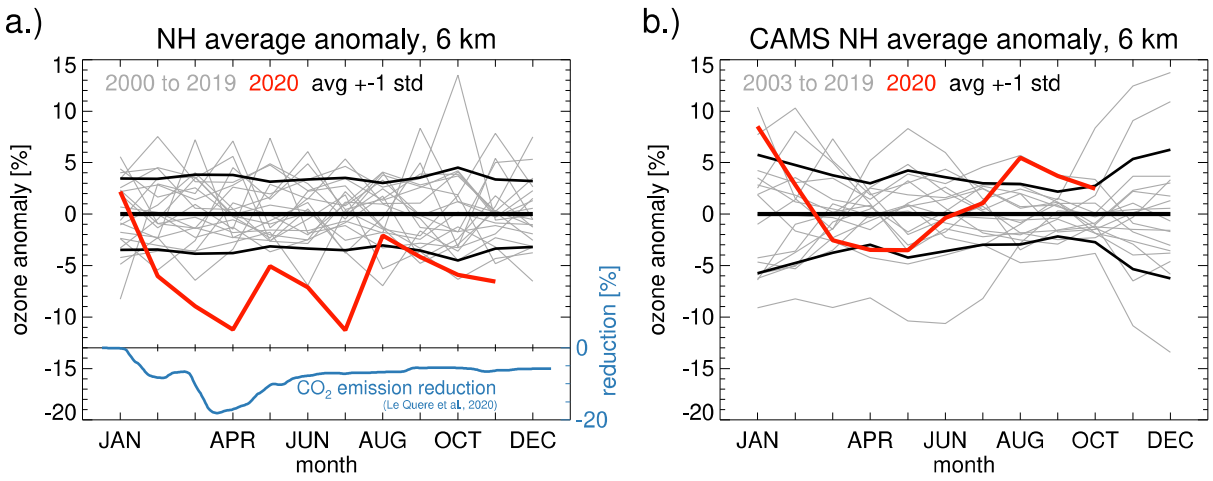

Figure 2. Annual cycles of monthly mean northern extratropical ozone anomalies at 6 km altitude. Anomalies are in percent, relative to the climatological monthly mean calculated for each station/ instrument, and for the period 2000 to 2020 (all Januaries, all Februaries, …, all Decembers). These single station/instrument anomalies are then averaged over all northern extratropical stations/instruments (north of 15°N). Panel **a)** Results from the station observations. Panel **b)** Results for CAMS atmospheric composition (re-)analyses at grid points nearest the stations. The CAMS data do not account for COVID-19 related emissions reductions in 2020. Grey lines: individual years from 2000 to 2019. Thick red line: year 2020. Thick black lines: average anomaly, ±1 standard deviation over the years. Dark blue lines and scale on the right in panel a): Global CO_2 emission reduction in 2020 (in percent) from Le Quéré et al. (2020b), as in Fig. 1.

Figs. 1 and 2 show large negative anomalies from April to August 2020. Fig. 3 compares anomaly profiles averaged over those five calendar months, between the years 2011 and 2020. Both years saw unusually large springtime ozone depletion in the Arctic stratosphere (Manney et al., 2020; Wohltmann et al., 2020). In the stratosphere, above ≈10 km, the Arctic depletion appears as low ozone, both in observations and CAMS results (particularly for stations north of 50°N). In both the stratosphere and the troposphere, the observed profiles show more variability than the smoother CAMS profiles. In 2020, most observed single station anomaly profiles (Fig. 3b) are negative throughout the northern extratropical troposphere (between 1 and 10 km). This is not the case in 2011 (Fig. 3a, 3c), nor in the CAMS data in 2020 (Fig. 3d).

The 2020 anomaly is even clearer for the northern extratropical mean profile (dark blue lines in Fig. 3). The observed 2020 mean anomaly profile is large, -6% to -9%, and statistically significant at the 95% level (more than 99% in fact) from 1 to 8 km (Fig. 3b), whereas the corresponding CAMS profile is close to zero (Fig. 3d). Fig. 3 indicates that Arctic stratospheric springtime ozone depletion did not have a large effect on tropospheric ozone below 8 km in 2011 and 2020 (see also Fig. S1 in the supplement), and that the CAMS “business as usual” simulation does not account for the observed large negative tropospheric anomaly in 2020.

Fig. 3b also shows a simulated profile of tropospheric ozone reduction from a recent chemistry-climate modelling study of COVID-like emissions decreases by Weber et al. (2020). This simulated profile (red line in our Fig 3b) matches the observed northern extratropical ozone reduction (dark blue line), from the ground up to about 8 km. Above 8 km, the simulated profile deviates by ≈10% from the observed profile, because it assumes fixed 2012 to 2014 meteorological conditions. The CAMS analyses (Fig. 3d) show that 2020 meteorological conditions and springtime Arctic stratospheric ozone depletion resulted in ozone reductions of 5% to 10% above 9 km, consistent with the observations.

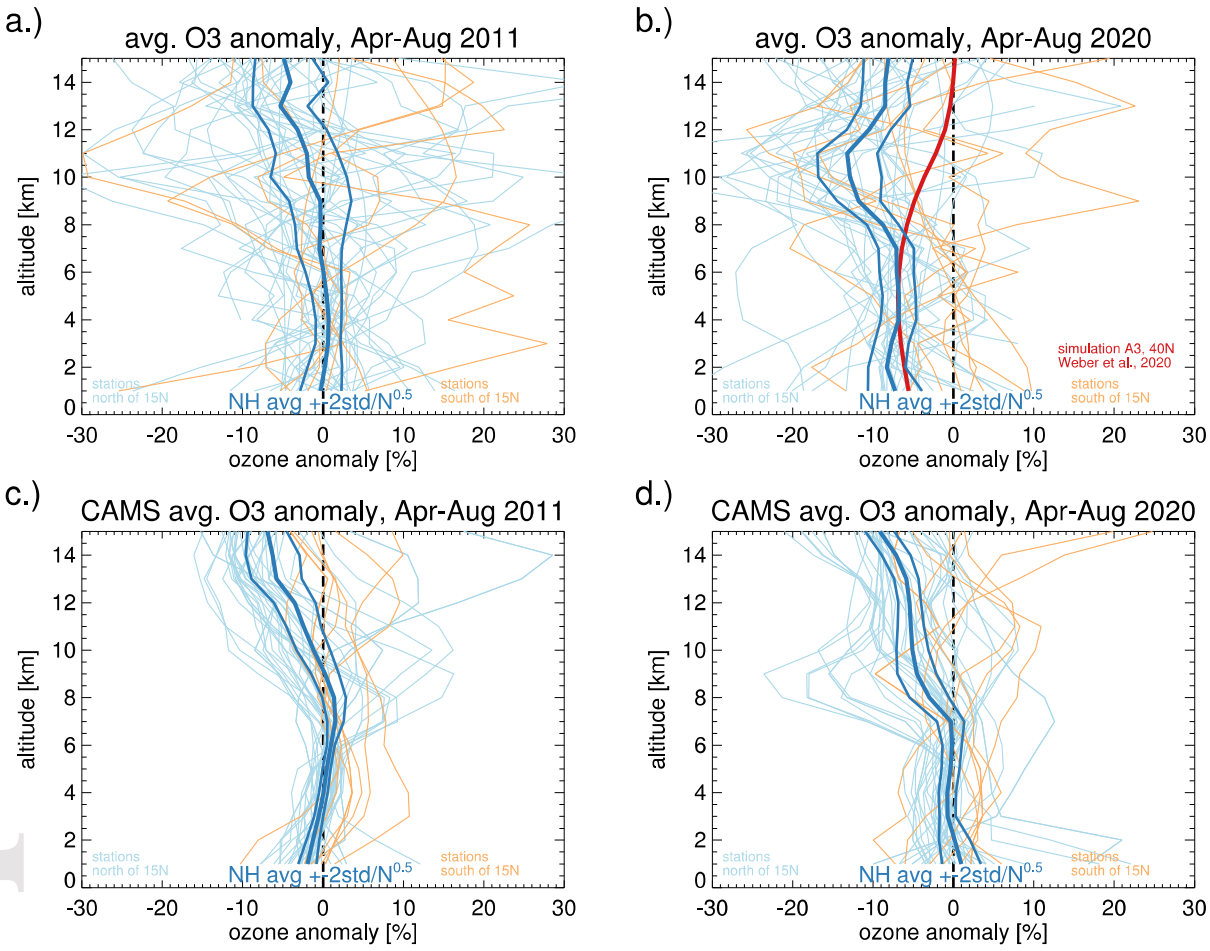

Figure 3. Ozone anomaly profiles (in percent), averaged over April to August. Stations are excluded in years where their data cover less than three of these five months. Panel **a)** for the year 2011. Panel **b)** for the year 2020. Light blue lines: northern extratropical stations (north of 15°N). Light orange lines: remaining stations, south of 15°N. Thick dark blue line: mean of the northern extratropical stations. Thin dark blue lines: 95% confidence interval of the mean of the northern extratropical stations. Red line in panel b): simulated ozone change at 40°N from Weber et al. (2020; Fig. S4, scenario A3). Panels **c), d)**: Same as a), b), but for CAMS (re-)analyses at the grid-points closest to the stations.

Time series of the tropospheric anomaly (averaged from April to August, and from 1 to 8 km altitude) are shown in Fig. 4. In the observations (left panel), the year 2020 stands out with large negative anomalies, not seen in the CAMS data. Across the twenty previous years, ozone anomalies at individual stations (thin lines) are scattered around zero. The northern extratropical average anomaly (dark blue line) is usually smaller than ±3%. The only other observed exception is the positive anomaly related to the (European) heat-wave summer of 2003 (Vautard et al., 2007). The large negative northern extratropical anomaly in the observations in 2020, ≈-7%, is clearly outside of the ±2σ range of the previous 20 years (thin dark blue lines). It is not reproduced by the CAMS "emissions as usual" analysis.

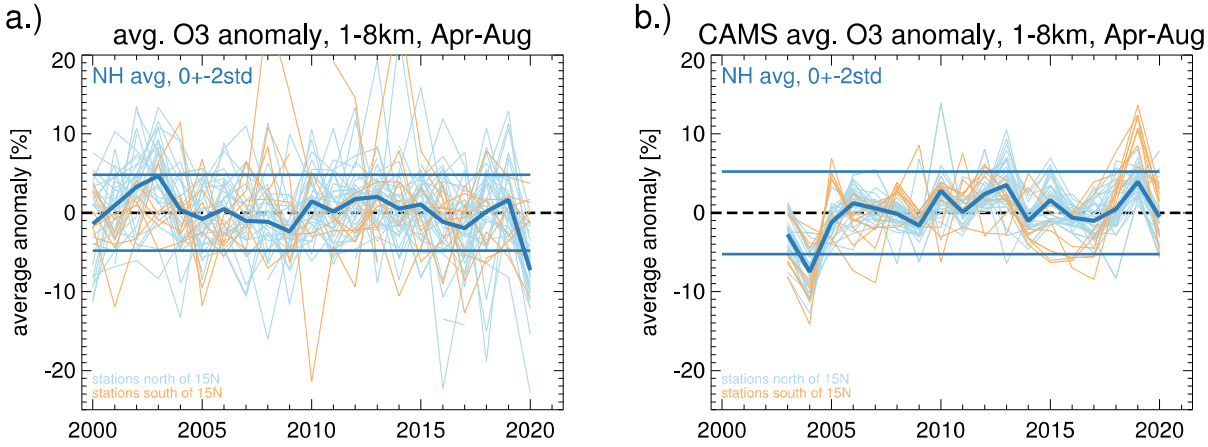

Figure 4. Tropospheric ozone anomaly, averaged over April to August and from 1 to 8 km, for the years 2000 to 2020. Panel **a)** Observations. Panel **b)** CAMS atmospheric composition (re-)analyses. Light blue lines: northern extratropical stations (north of 15°N). Light orange lines: stations south of 15°N. Thick dark blue line: Average over all stations north of 15°N. Thin dark blue lines: ±2 standard deviations over all years of this average.

The geographic distribution of the average tropospheric ozone anomalies is shown for 2011 and 2020 in Fig. 5. 2020 stands out in the observations with large negative anomalies at nearly all northern extratropical stations, and a fairly uniform geographical distribution (see Table S1 of the supplement for the numerical values). CAMS does show negative anomalies in 2020, but only north of 50°N, and not as large as the observations. In the Southern Hemisphere in 2020, agreement between observations and CAMS is quite good, typically within 2.5% or better (see also Table S1 in supplement). In 2011, some stations show positive anomalies, negative anomalies are not as large as in 2020, and the geographical distribution is less uniform. Agreement between observations and CAMS is reasonable in 2011, usually within a few percent.

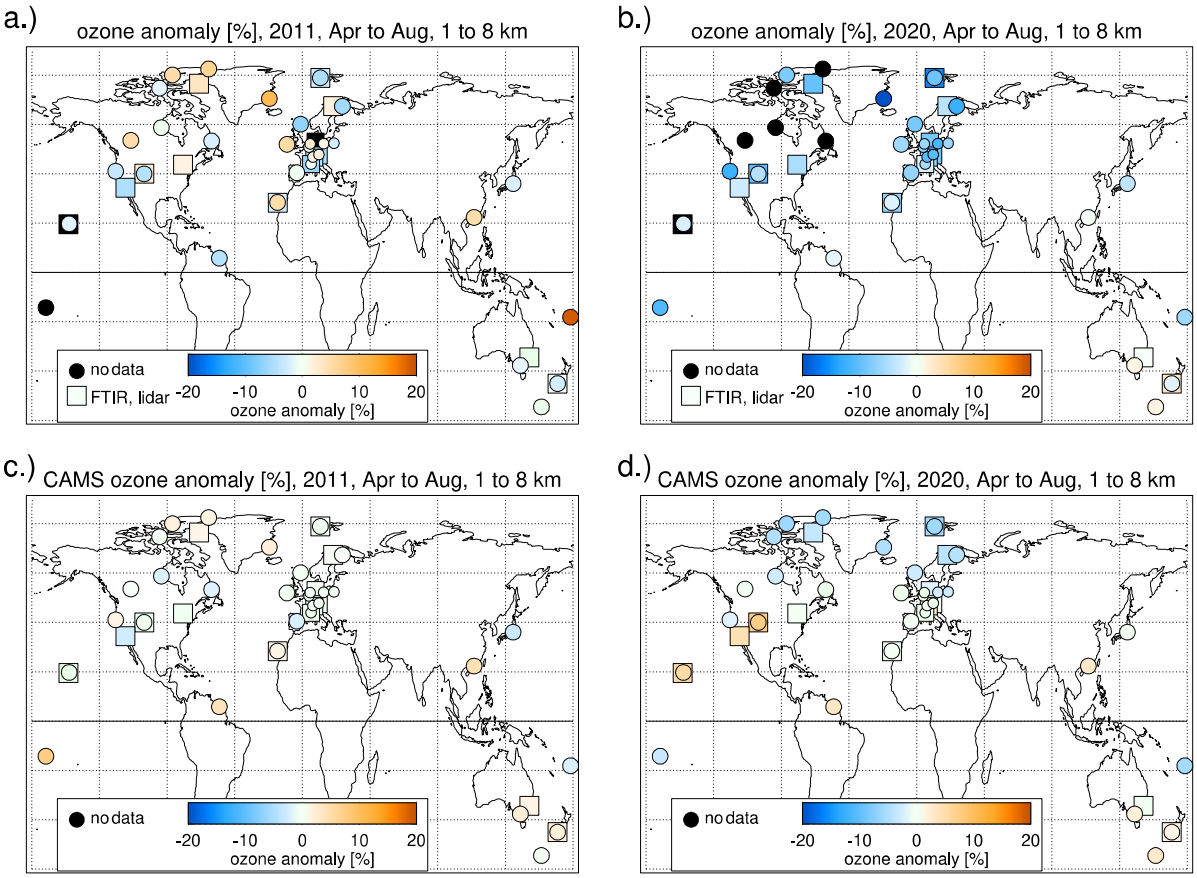

Figure 5. Geographic distribution of observed tropospheric ozone anomalies (averaged over the months April to August, and over altitudes from 1 to 8 km) for the years **a)** 2011 and **b)** 2020. Panels **c)** and **d):** same, but for CAMS results at the station locations. Colored circles give the anomaly at the ozonesonde stations. Squares are for FTIR and lidar stations. See Table S1 of the supplement for the numerical values. Black filling indicates insufficient data in the given year.

4 Discussion and Conclusions

Ozone stations in the northern extratropics indicate exceptionally low ozone in the free troposphere (1 to 8 km) in spring and summer 2020. Compared to the 2000-2020 climatology, ozone was reduced by 7% (≈4 nmol/mol). Such widespread low tropospheric ozone, across so many stations and over several months has not been observed in any previous year since 2000. The observed 7% ozone reduction in the free troposphere stands in contrast to increases of surface ozone by 10% to 30%, reported for many polluted urban areas after the COVID-19 related emissions reductions in 2020 (e.g., Collivignarelli et al., 2020; Lee et al., 2020; Shi & Brasseur, 2020; Siciliano et al., 2020; Venter et al., 2020). However, the chemical regime for ozone in the free troposphere is different (e.g., Kroll et al., 2020; Sillman, 1999; Thornton et al., 2002), and free tropospheric ozone reductions are expected after the substantial decrease of precursor emissions due to the COVID-19 pandemic (e.g. Guevara et al., 2020; Zhang et al., 2020).

Recent model simulations of COVID-like emissions decreases (Weber et al., 2020) find tropospheric ozone reductions very similar to our observational results. From our results, and the simulations by Weber et al., 2020, it appears that the total tropospheric ozone burden of the northern extratropics decreased by about 7% for April to August 2020. The contribution from ozone increases in polluted urban areas to the total burden is opposite, but very small.

The Weber et al. (2020) simulations indicate that the major causes of tropospheric ozone reduction come from reduced surface transportation (ozone decrease throughout most of the northern extratropical troposphere), and from reduced aviation (ozone decrease mostly between 10 and 12 km altitude and north of 30°N, see also Grewe et al., 2017). While the simulations are qualitatively consistent with the observations, they consider only March to May. New simulations using more recent and extended emissions estimates (Le Quéré et al., 2020b; Liu at al., 2020), and further comparison with our station observations would be worthwhile.

The observed large and fairly uniform 7% reduction of ozone in the northern extratropical troposphere in spring and summer 2020 provides a far reaching test case for the response of tropospheric ozone to emission changes. Further quantification of this anomaly will be possible, when observations from commercial aircraft (IAGOS), and satellite instruments become available. Additional modelling studies will improve our understanding of the contributions from different sectors such as air traffic, and surface transportation.

Acknowledgments

The authors greatly acknowledge the know-how and the hard work of station personnel launching the ozonesondes and taking the ground-based measurements. Without their dedicated efforts over many years, and especially during the COVID-19 lockdowns in 2020, investigations like this one are not possible!

Funding acknowledgments

Deutscher Wetterdienst funds the ozone program at Hohenpeißenberg and makes research like this possible.

NOAA GML supported additional launches in Boulder and Trinidad Head in April and May 2020. NOAA and NASA's Upper Atmosphere Composition Observations (UACO) Program support the SHADOZ ozone soundings at Hilo, Pago-Pago (American Samoa) and Suva (Fiji). UACO also provides partial support for the Boulder FTIR and the Table Mountain Lidar.

The NDACC FTIR stations Bremen, Ny□Ålesund, Izaña, Kiruna, and Zugspitze have been supported by the German Bundesministerium für Wirtschaft und Energie (BMWi) via DLR under grants 50EE1711A, 50EE1711B, and 50EE1711D. Izaña, Kiruna, and Zugspitze have also been supported by the Helmholtz Society via the research program ATMO.

The FTIR measurements in Bremen and Ny-Ålesund receive additional support by the Senate of Bremen, the FTIR measurements in Ny-Ålesund also by AWI Bremerhaven. The University of Bremen further acknowledges funding by DFG (German research foundation) TRR 172 – Project Number 268020496 – within the Transregional Collaborative Research Center "ArctiC

Amplification: Climate Relevant Atmospheric and SurfaCe Processes, and Feedback Mechanisms (AC)3".

The University of Liège contribution has been supported primarily by the Fonds de la Recherche Scientifique - FNRS under grant J.0147.18, as well as by the CAMS project. EM is a senior research associate of the F.R.S.-FNRS.

The Toronto FTIR measurements were supported by Environment and Climate Change Canada, the Natural Sciences and Engineering Research Council of Canada (NSERC), and the NSERC CREATE Training Program in Technologies for Exo-Planetary Science.

The University of the Wollongong thanks the Australian Research Council that has provided significant support over the years for the NDACC site at Wollongong, most recently as part of project DP160101598.

Part of this research work was carried out at the Jet Propulsion Laboratory, California Institute of Technology, under a contract with the National Aeronautics and Space Administration (80NM0018D004).

The National Center for Atmospheric Research is sponsored by the National Science Foundation. The NCAR FTS observation programs at Thule, GR and Boulder, CO are supported under contract by the National Aeronautics and Space Administration (NASA). The Thule work is also supported by the NSF Office of Polar Programs (OPP). We wish to thank the Danish Meteorological Institute for support at the Thule site and NOAA for support of the MLO site.

Key results for this manuscript were generated using Copernicus Atmosphere Monitoring Service Information from the European Community.

No author reports a financial (or other) conflict of interest.

Data Sources

Most of the ozonesonde data used in this study are freely available from the World Ozone and UV Data Centre (https://woudc.org) at Environment Canada (https://exp-studies.tor.ec.gc.ca/), and are downloadable at https://woudc.org/archive/Archive-NewFormat/OzoneSonde_1.0_1/).

Some ozonesonde data for 2020 were not yet available at the WOUDC. Instead, rapid delivery data were obtained from ftp://zardoz.nilu.no/nadir/projects/vintersol/data/o3sondes (requires registration), at the Nadir database of the Norwegian Institute for Air Quality (NILU, https://projects.nilu.no/nadir/obs.html). Registration information, and the same data in a different format, are available from the European Space Agency Validation Data Center (https://evdc.esa.int/).

For Boulder, Trinidad Head, Hilo, Fiji, and Samoa, stations operated by the US National Oceanic and Atmospheric Administration, Global Monitoring Laboratory (https://www.esrl.noaa.gov/gmd/ozwv/), data can be obtained freely from ftp://aftp.cmdl.noaa.gov/data/ozwv/Ozonesonde/ .

FTIR and lidar data, as well as some ozonesonde data, are from the Network for the Detection of Atmospheric Composition Change (https://ndacc.org), and are freely available at ftp://ftp.cpc.ncep.noaa.gov/ndacc/station/ and ftp://ftp.cpc.ncep.noaa.gov/ndacc/RD/.

Copernicus Atmosphere Monitoring Service (CAMS) global chemical weather EAC4 re-analyses are available at https://atmosphere.copernicus.eu/data . CAMS operational global analyses and forecasts are available at https://apps.ecmwf.int/datasets/data/cams-nrealtime/ .

References

Archibald, A.T., Neu, J.L., Elshorbany, Y., Cooper, O.R., Young, P.J., Akiyoshi, H., et al. (2020). Tropospheric Ozone Assessment Report: A critical review of changes in the tropospheric ozone burden and budget from 1850-2100. *Elementa Science of the Anthropocene*, **8**, 034. https://doi.org/10.1525/elementa.2020.034

Barré, J., Petetin, H., Colette, A., Guevara, M., Peuch, V.-H., Rouil, L., et al. (in review, 2020). Estimating lockdown induced European NO_2 changes. *Atmospheric Chemistry and Physics Discussions*. https://doi.org/10.5194/acp-2020-995

Bauwens, M., Compernolle, S., Stavrakou, T., Müller, J.□F., van Gent, J., Eskes, H., et al. (2020). Impact of coronavirus outbreak on NO_2 pollution assessed using TROPOMI and OMI observations. *Geophysical Research Letters*, **47**, e2020GL087978. https://doi.org/10.1029/2020GL087978

Bozem, H., Butler, T. M., Lawrence, M. G., Harder, H., Martinez, M., Kubistin, D., et al. (2017). Chemical processes related to net ozone tendencies in the free troposphere. *Atmospheric Chemistry and Physics*, **17**, 10565–10582, https://doi.org/10.5194/acp-17-10565-2017

Chen, L.-W. A., Chien, L.-C., Li, Y., and Lin, G. (2020). Nonuniform impacts of COVID-19 lockdown on air quality over the United States, *Science of The Total Environment*, **745**, 141105. https://doi.org/10.1016/j.scitotenv.2020.141105

Collivignarelli, M.C., Abbà, A., Bertanza, G., Pedrazzani, R., Ricciardi, P., & Carnevale Miino, M. (2020). Lockdown for CoViD-2019 in Milan: What are the effects on air quality? *Science of the Total Environment*, **732**, 139280. https://doi.org/10.1016/j.scitotenv.2020.139280

Cooper, O.R., Parrish, D.D., Ziemke, J., Balashov, N.V., Cupeiro, M., Galbally, I.E., et al. (2014). Global distribution and trends of tropospheric ozone: An observation-based review. *Elementa: Science of the Anthropocene*, **2**, 000029. https://doi.org/10.12952/journal.elementa.000029

De Mazière, M., Thompson, A. M., Kurylo, M. J., Wild, J. D., Bernhard, G., Blumenstock, T., et al. (2018). The Network for the Detection of Atmospheric Composition Change (NDACC): history, status and perspectives. *Atmospheric Chemistry and Physics*, **18**, 4935–4964. https://doi.org/10.5194/acp-18-4935-2018

Dentener F., T. Keating, T., & Akimoto, H. (eds.) (2011). *Hemispheric Transport of Air Pollution 2010, Part A: Ozone and Particulate Matter*. Air Pollution Studies No. 17, United Nations, New York and Geneva, ISSN 1014-4625, ISBN 978-92-1-117043-6. [Available online at http://www.unece.org/index.php?id=25381]

Ding, J., van der A, R. J., Eskes, H. J., Mijling, B., Stavrakou, T., van Geffen, J. H. et al. (2020). NO_x emissions reduction and rebound in China due to the COVID□19 crisis. *Geophysical Research Letters*, **46**, e2020GL089912. https://doi.org/10.1029/2020GL089912

Feng, S., Jiang, F., Wang, H., Wang, H., Ju, W., Shen, Y., et al. (2020). NO_x emission changes over China during the COVID□19 epidemic inferred from surface NO_2 observations. *Geophysical Research Letters*, **47**, e2020GL090080. https://doi.org/10.1029/2020GL090080

Gaudel, A., Ancellet, G., & Godin-Beekmann, S. (2015). Analysis of 20 years of tropospheric ozone vertical profiles by lidar and ECC at Observatoire de Haute Provence (OHP) at 44°N, 6.7°E. *Atmospheric Environment*, **113**, 78-89. https://doi.org/10.1016/j.atmosenv.2015.04.028

Gaudel, A., Cooper, O.R., Ancellet, G., Barret, B., Boynard, A., Burrows, J.P., et al. (2018). Tropospheric Ozone Assessment Report: Present-day distribution and trends of tropospheric ozone relevant to climate and global atmospheric chemistry model evaluation. *Elementa Science of the Anthropocene*, **6**, 39. https://doi.org/10.1525/elementa.291

Gelaro, R., McCarty, W., Suarez, M. J., Todling, R., Molod, A., Takacs, et al. (2017). The Modern□Era Retrospective Analysis for Research and Applications, version 2 (MERRA□2). *Journal of Climate*, **30**, 5419–5454. https://doi.org/10.1175/JCLI-D-16-0758.1

Goldberg, D. L., Anenberg, S. C., Griffin, D., McLinden, C. A., Lu, Z., & Streets, D. G. (2020). Disentangling the impact of the COVID□19 lockdowns on urban NO_2 from natural variability. *Geophysical Research Letters*, **47**, e2020GL089269. https://doi.org/10.1029/2020GL089269

Granados-Muñoz, M. J., & Leblanc, T. (2016). Tropospheric ozone seasonal and long-term variability as seen by lidar and surface measurements at the JPL-Table Mountain Facility, California. *Atmospheric Chemistry and Physics*, **16**, 9299–9319. https://doi.org/10.5194/acp-16-9299-2016

Grewe, V., Dahlmann, K., Flink, J., Frömming, C., Ghosh, R., Gierens, et al. (2017). Mitigating the Climate Impact from Aviation: Achievements and Results of the DLR WeCare Project. *Aerospace*, **4**, 34, https://doi.org/10.3390/aerospace4030034

Guevara, M., Jorba, O., Soret, A., Petetin, H., Bowdalo, D., Serradell, K., et al. (2020, accepted). Time-resolved emission reductions for atmospheric chemistry modelling in Europe during the COVID-19 lockdowns. *Atmospheric Chemistry and Physics.* https://doi.org/10.5194/acp-2020-686

Hurtmans, D., Coheur, P.-F., Wespes, C., Clarisse, L., Scharf, O., Clerbaux, C., et al. (2012). FORLI radiative transfer and retrieval code for IASI. *Journal of Quantitative Spectroscopy and Radiative Transfer*, **113** (11), 1391-1408. https://doi.org/10.1016/j.jqsrt.2012.02.036.

Inness, A., Ades, M., Agusti-Panareda, A., Barré, J., Benedictow, A., Blechschmidt, A.M., et al. (2019). The CAMS reanalysis of atmospheric composition. *Atmospheric Chemistry and Physics*, **19**, 3515–3556. https://doi.org/10.5194/acp-19-3515-2019

Keller, C. A., Evans, M. J., Knowland, K. E., Hasenkopf, C. A., Modekurty, S., Lucchesi, et al. (accepted, 2021). Global Impact of COVID-19 Restrictions on the Surface Concentrations of Nitrogen Dioxide and Ozone. *Atmospheric Chemistry and Physics Discussions.* https://doi.org/10.5194/acp-2020-685

Kroll, J.H., Heald, C.L., Cappa, C.D., Farmer, D.K., Fry, J.L., Murphy, J.G., & Steiner, A.L. (2020). The complex chemical effects of COVID-19 shutdowns on air quality. *Nature Chemistry*, **12**, 777–779. https://doi.org/10.1038/s41557-020-0535-z

Leblanc, T., Brewer, M. A., Wang, P. S., Granados-Muñoz, M. J., Strawbridge, K. B., Travis, M., et al. (2018). Validation of the TOLNet lidars: the Southern California Ozone Observation Project (SCOOP). *Atmospheric Measurement Techniques*, **11**, 6137–6162. https://doi.org/10.5194/amt-11-6137-2018

Lee, J. D., Drysdale, W. S., Finch, D. P., Wilde, S. E., & Palmer, P. I. (2020). UK surface NO_2 levels dropped by 42 % during the COVID-19 lockdown: impact on surface O3, *Atmospheric Chemistry and Physics*, **20**, 15743–15759. https://doi.org/10.5194/acp-20-15743-2020

Le Quéré, C., Jackson, R.B., Jones, M.W., Smith, A.J.P., Abernethy, S., Andrew, R.M., et al. (2020a). Temporary reduction in daily global CO_2 emissions during the COVID-19 forced confinement. *Nature Climate Change*, **10**, 647-653. https://doi.org/10.1038/s41558-020-0797-x

Le Quéré, C., Jackson, R.B., Jones, M.W., Smith, A.J.P., Abernethy, S., Andrew, R.M., et al. (2020b). Supplementary data to: Le Quéré et al (2020), Temporary reduction in daily global CO_2 emissions during the COVID-19 forced confinement (Version 1.2). *Global Carbon Project*. https://doi.org/10.18160/RQDW-BTJU

Liu, X., Bhartia, P. K., Chance, K., Spurr, R.J.D., & Kurosu, T. P. (2010). Ozone profile retrievals from the Ozone Monitoring Instrument. *Atmospheric Chemistry and Physics*, **10**, 2521–2537. https://doi.org/10.5194/acp-10-2521-2010

Liu, Z., Ciais, P., Deng, Z., Lei, R., Davis, S. J., Feng, S., et al. (2020). Near-real-time monitoring of global CO_2 emissions reveals the effects of the COVID-19 pandemic. *Nature Communications*, **11**, 5172. https://doi.org/10.1038/s41467-020-18922-7

Manney, G. L., Livesey, N. J., Santee, M. L., Froidevaux, L., Lambert, A., Lawrence, Z. D., et al. (2020). Record□low Arctic stratospheric ozone in 2020: MLS observations of chemical processes and comparisons with previous extreme winters. *Geophysical Research Letters*, **47**, e2020GL089063. https://doi.org/10.1029/2020GL089063

Menut, L., Bessagnet, B., Siour, G., Mailler, S., Pennel, R., & Cholakian, A. (2020). Impact of lockdown measures to combat Covid-19 on air quality over western Europe. *Science of The Total Environment*, **741**, 140426. https://doi.org/10.1016/j.scitotenv.2020.140426

Nédélec, P., Blot, R., Boulanger, D., Athier, G., Cousin, J-M., Gautron, B., et al. (2015). Instrumentation on commercial aircraft for monitoring the atmospheric composition on a global scale: the IAGOS system, technical overview of ozone and carbon monoxide measurements. *Tellus B: Chemical and Physical Meteorology*, **67**(1). https://doi.org/10.3402/tellusb.v67.27791

Neu, J., Flury, T., Manney, G., Santee, M.L., Livesey N.J., & Worden, J. (2014). Tropospheric ozone variations governed by changes in stratospheric circulation. *Nature Geosci*ence, **7**, 340–344. https://doi.org/10.1038/ngeo2138

Oetjen, H., Payne, V. H., Kulawik, S. S., Eldering, A., Worden, J., Edwards, D. P., et al. (2014). Extending the satellite data record of tropospheric ozone profiles from Aura-TES to MetOp-IASI: characterisation of optimal estimation retrievals. *Atmospheric Measurement Techniques*, **7**, 4223–4236. https://doi.org/10.5194/amt-7-4223-2014

Ordóñez, C., Garrido-Perez, J.M., & García-Herrera, R. (2020). Early spring near-surface ozone in Europe during the COVID-19 shutdown: Meteorological effects outweigh emission changes. *Science of the Total Environment*, **747**, 141322. https://doi.org/10.1016/j.scitotenv.2020.141322

Park, S., Son, S.-W., Jung, M.-I., Park, J., & Park, S.-S. (2020). Evaluation of tropospheric ozone reanalyses with independent ozonesonde observations in East Asia. *Geoscience Letters*. **7**, 12. https://doi.org/10.1186/s40562-020-00161-9

Parrish, D.D., Derwent, R.G., Steinbrecht, W., Stübi, R., Van Malderen, R., Steinbacher, M., et al. (2020). Zonal similarity of long□term changes and seasonal cycles of baseline ozone at northern midlatitudes. *Journal of Geophysical Research: Atmospheres*, **125**, e2019JD031908. https://doi.org/10.1029/2019JD031908

Sicard, P., De Marco, A., Agathokleous, E., Feng, Z., Xu, X., Paoletti, E., et al. (2020). Amplified ozone pollution in cities during the COVID-19 lockdown, *Science of the Total Environment*, **735**, 139542. https://doi.org/10.1016/j.scitotenv.2020.139542

Siciliano, B., Dantas, G., da Silva, C. M., & Arbilla G. (2020). Increased ozone levels during the COVID-19 lockdown: Analysis for the city of Rio de Janeiro, Brazil, *Science of the Total Environment*, **737**, 139765. https://doi.org/10.1016/j.scitotenv.2020.139765

Sillman, S., (1999). The relation between ozone, NO_x and hydrocarbons in urban and polluted rural environments. *Atmospheric Environment*, **33**(12), 1821-1845. https://doi.org/10.1016/S1352-2310(98)00345-8

Shi, X., & Brasseur, G. P. (2020). The response in air quality to the reduction of Chinese economic activities during the COVID□19 outbreak. *Geophysical Research Letters*, **47**, e2020GL088070. https://doi.org/10.1029/2020GL088070

Smit, H.G.J., Straeter, W., Johnson, B., Oltmans, S., Davies, J., Tarasick, D.W., et al. (2007). Assessment of the performance of ECC-ozonesondes under quasi-flight conditions in the environmental simulation chamber: Insights from the Jülich Ozone Sonde Intercomparison Experiment (JOSIE). *Journal of Geophysical Research*, **112**, D19306. https://doi.org/10.1029/2006JD007308

Stauffer, R.M., Thompson, A.M., Kollonige, D.E., Witte, J.C., Tarasick, D.W., Davies, J., et al. (2020). A post□2013 dropoff in total ozone at a third of global ozonesonde stations: Electrochemical concentration cell instrument artifacts? *Geophysical Research Letters*, **47**, e2019GL086791. https://doi.org/10.1029/2019GL086791

Sterling, C.W., Johnson, D.J., Oltmans, S.J., Smit, H.G.J., Jordan, A.F., Cullis, P.D., et al. (2018). Homogenizing and estimating the uncertainty in NOAA's long-term vertical ozone profile records measured with the electrochemical concentration cell ozonesonde. *Atmospheric Measurement Techniques*, **11**, 3661-3687. https://doi.org/10.5194/amt-11-3661-2018

Strahan, S. E., Douglass, A. R., & Damon, M. R. (2019). Why do Antarctic ozone recovery trends vary? *Journal of Geophysical Research: Atmospheres*, **124**, 8837–8850. https://doi.org/10.1029/2019JD030996

Tarasick, D.W., Davies, J., Smit, H.G.J., & Oltmans, S.J. (2016). A re-evaluated Canadian ozonesonde record: measurements of the vertical distribution of ozone over Canada from 1966 to 2013. *Atmospheric Measurement Techniques*, **9**, 195-214. https://doi.org/10.5194/amt-9-195-2016.

Tarasick, D., Galbally, I.E., Cooper, O.R., Schultz, M.G., Ancellet, G., Leblanc, T., et al. (2019). Tropospheric Ozone Assessment Report: Tropospheric ozone from 1877 to 2016, observed

levels, trends and uncertainties. *Elementa Science of the Anthropocene*, **7**(1). https://doi.org/10.1525/elementa.376

Thornton, J.A., Wooldridge, P.J., Cohen, R.C., Martinez, M., Harder, H., Brune, W. H., et al. (2002). Ozone production rates as a function of NO_x abundances and HO_x production rates in Nashville urban plume. *Journal of Geophysical Research*, **107** (D12). https://doi.org/10.1029/2001JD000932

Van Malderen, R., Allaart, M. A. F., De Backer, H., Smit, H. G. J., & De Muer, D. (2016). On instrumental errors and related correction strategies of ozonesondes: possible effect on calculated ozone trends for the nearby sites Uccle and De Bilt. *Atmospheric Measurement Techniques*, **9**, 3793–3816. https://doi.org/10.5194/amt-9-3793-2016

Vautard, R., Beekmann, M., Desplat, J., Hodzic, A., & Morel, S. (2007). Air quality in Europe during the summer of 2003 as a prototype of air quality in a warmer climate. *Comptes Rendus Geoscience*, **339**, 747-763. https://doi.org/10.1016/j.crte.2007.08.003

Venter, Z. S., Aunan, K., Chowdhury, S., & Lelieveld, J. (2020). COVID-19 lockdowns cause global air pollution declines. *Proceedings of the National Academy of Sciences*, **117** (32), 18984-18990. https://doi.org/10.1073/pnas.2006853117

Vigouroux, C, Blumenstock, T, Coffey, M, Errera, Q, García, O, Jones, N.B, et al. (2015). Trends of ozone total columns and vertical distribution from FTIR observations at eight NDACC stations around the globe. *Atmospheric Chemistry and Physics*, **15**, 2915–2933. https://doi.org/10.5194/acp-15-2915-2015

Weber, J., Shin, Y. M., Staunton Sykes, J., Archer□Nicholls, S., Abraham, N. L., & Archibald, A. T. (2020). Minimal climate impacts from short□lived climate forcers following emission reductions related to the COVID□19 pandemic. *Geophysical Research Letters*, **47**, e2020GL090326. https://doi.org/10.1029/2020GL090326

Witte, J. C., Thompson, A.M., Smit, H.G.J., Fujiwara, M., Posny, F., Coetzee G.J.R., et al. (2017). First reprocessing of Southern Hemisphere ADditional OZonesondes (SHADOZ) profile records (1998–2015): 1. Methodology and evaluation. *Journal of Geophysical Research: Atmospheres*, **122**, 6611– 6636. https://doi.org/10.1002/2016JD026403

WMO (2014), *Quality assurance and quality control for ozonesonde measurements in GAW,* World Meteorological Organization (WMO), Global Atmosphere Watch report series, Smit, H.G.J., and ASOPOS panel (eds.), GAW Report No. 201, 100 pp., Geneva. [Available online at https://library.wmo.int/doc_num.php?explnum_id=7167]

Wohltmann, I., von der Gathen, P., Lehmann, R., Maturilli, M., Deckelmann, H., Manney, G. L., et al. (2020). Near□complete local reduction of Arctic stratospheric ozone by severe chemical loss in spring 2020. *Geophysical Research Letters*, **47**, e2020GL089547. https://doi.org/10.1029/2020GL089547

Wu, S., Mickley, L. J., Jacob, D. J., Logan, J. A., Yantosca, R. M., & Rind, D. (2007). Why are there large differences between models in global budgets of tropospheric ozone? *Journal of Geophysical Research*, **112**, D05302. https://doi.org/10.1029/2006JD007801

Zhang, Y., West, J. J., Emmons, L. K., Flemming, J., Jonson, J. E., Lund, M. T., et al. (2020). Contributions of world regions to the global tropospheric ozone burden change from 1980 to

2010. *Geophysical Research Letters*, **47**, e2020GL089184.
https://doi.org/10.1029/2020GL089184